Preprint Title Entry to 2-Aminoprolines via Electrochemical Decarboxylative Amidation of *N*-Acetylamino Malonic Acid Monoesters

Authors Olesja Koleda, Janis Sadauskis, Darja Antonenko, Edvards Janis Treijs, Raivis Davis Steberis and Edgars Suna

Publication Date 19 Dez. 2024

Article Type Full Research Paper

Supporting Information File 1 Koleda_SI_final.pdf; 13.3 MB

ORCID® iDs Olesja Koleda - https://orcid.org/0000-0002-5173-8561; Janis Sadauskis - https://orcid.org/0009-0002-6962-7621; Raivis Davis Steberis - https://orcid.org/0009-0001-2610-0208; Edgars Suna - https://orcid.org/0000-0002-3078-0576

Entry to 2-Aminoprolines via Electrochemical Decarboxylative Amidation of *N*-Acetylamino Malonic Acid Monoesters

Olesja Koleda[1,2], Janis Sadauskis[1,2], Darja Antonenko[1,2], Edvards Janis Treijs[1,2], Raivis Davis Steberis[1,2] and Edgars Suna*[1,2]

[1] Latvian Institute of Organic Synthesis, Aizkraukles 21, Riga LV-1006, Latvia

[2] Faculty of Medicine and Life Sciences, Department of Chemistry, University of Latvia, Jelgavas 1, Riga LV-1004, Latvia

edgars@osi.lv

Abstract. Electrochemical synthesis of 2-aminoprolines capitalizes on anodic decarboxylation-intramolecular amidation of readily available *N*-acetylamino malonic acid monoesters. The decarboxylative amidation under Hofer–Moest reaction conditions proceeds in an undivided cell under constant current conditions in aqueous acetonitrile and provides an access to *N*-sulfonyl, *N*-benzoyl, and *N*-Boc-protected 2-aminoproline derivatives.

Graphical Abstract

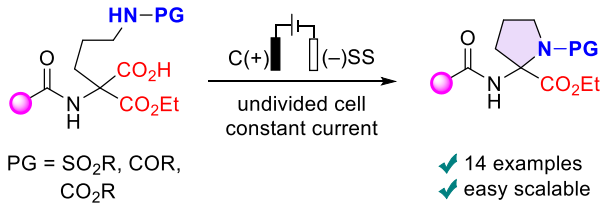

Keywords.

Anodic oxidation; decarboxylation; electrosynthesis; Hofer-Moest reaction, non-proteinogenic amino acids

* Corresponding author

Introduction

Non-proteinogenic cyclic amino acids are common structural motifs in design of small-molecule drugs and peptidomimetics [1]. For example, clinically used anesthetics carfentanil **1** and remifentanil **2**, FDA-approved antipruritic medication defelikefalin **3**, and arginase inhibitor **4** [2] possess cyclic α,α-disubstituted piperidine-containing amino acid subunits. Likewise, cyano-substituted cyclic aminal is a core structure of fibroblast activation protein inhibitor **5** [3] (Figure 1). The widespread use of non-proteinogenic cyclic amino acids in drug discovery justifies both the design of new analogs and the development of efficient synthetic methods to access these medicinally relevant structural motifs. Herein we report on electrochemical synthesis of 2-aminoproline and 2-amino pipecolic acid derivatives **6** (Figure 1).

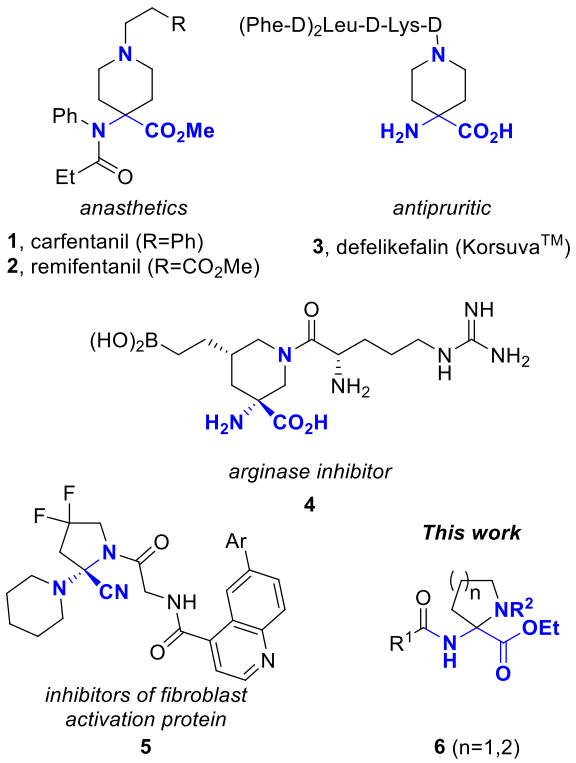

Figure 1. Selected examples of α,α-disubstituted cyclic amino acids in drug design

Recently we disclosed electrochemical approach to tetrahydrofuran and tetrahydropyran-containing amino acid derivatives via anodic decarboxylation of *N*-acetylamino malonic acid monoesters to generate a stabilized carbocation (Hofer-Moest conditions), which then reacted with a tethered oxygen nucleophile [4]. In this follow-up study, we demonstrate that *N*-protected amines are also suitable as nucleophiles for the cyclization into 2-aminoproline and 2-amino pipecolic acid derivatives **6** (Figure 2,

eq 3). The starting disubstituted malonic esters are readily available by *C*-alkylation of inexpensive and readily available diethyl acetamidomalonate, followed by monohydrolysis under basic conditions. The electrolysis proceeds in an undivided cell under galvanostatic control using low-cost graphite or stainless-steel electrodes, and the protocol was easily upscaled. Notably, excellent diastereoselectivity (97:3 d.r.) could be achieved in the cyclization of tethered chiral nitrogen nucleophile as shown below. To the best of our knowledge, the electrosynthesis of *gem*-α,α-diamino acid derivatives **6** is not precedented, and all published electrochemical amination examples under Hofer-Moest conditions [5] targeted either *N*-substituted heteroarenes [6] or aminals [7,8] (Figure 2, eq 1 and 2, respectively).

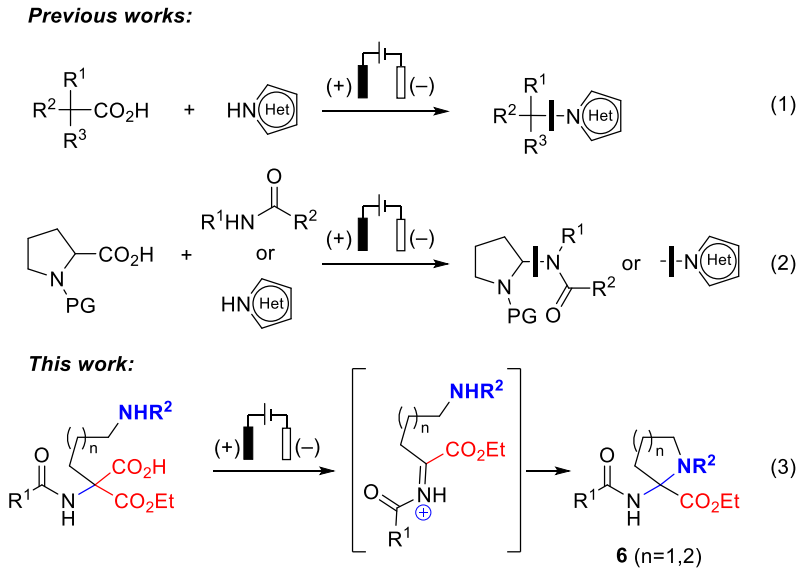

Figure 2. Electrochemical decarboxylative amination.

Results and Discussion

N-Acetylamino malonic acid monoester **9a** possessing tosyl-protected tethered amine was selected as a model substrate for the development of intramolecular amidation under Hofer-Moest conditions. The acid **9a** was prepared in three steps (62% overall yield) from commercially available diethyl acetamidomalonate by an alkylation/hydrolysis/Boc-cleavage sequence (Scheme 1).

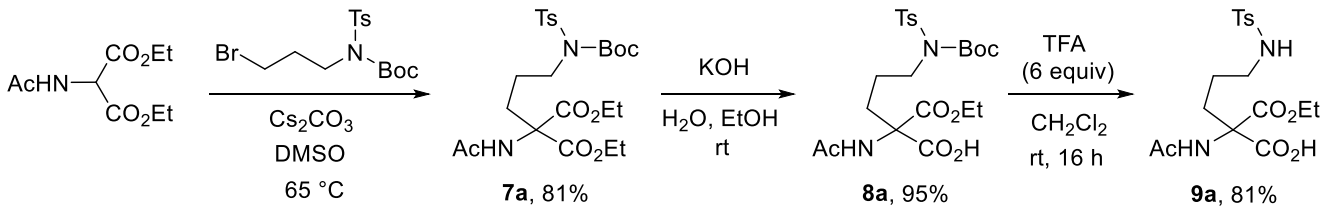

Scheme 1. Preparation of malonic acid monoester **9a**.

Development of decarboxylative amidation commenced by examining the published conditions for anodic decarboxylation/etherification [4]. Accordingly, the electrolysis of monoester **9a** in 2:1 MeCN:H_2O mixture in the presence of 0.025 M $LiClO_4$ solution under constant current conditions (j = 12 mA/cm^2) with graphite both as an anode and a cathode material afforded the desired *N*-tosyl pyrrolidine **6a** in 67% yield (Table 1, entry 1). The water quench of a transient *N*-acyliminium species was found to be major side-reaction as evidenced by the formation of an open-chain hemiaminal **10a** (the hemiaminal could not be isolated due to the instability on silica gel). Screening of other supporting electrolytes revealed that basic salts (K_2CO_3, Na_2CO_3, NaOAc) do not improve the efficiency of anodic decarboxylation/cyclization reaction (entries 2–4). Even though the amount of hemiaminal **10a** was slightly reduced, the formation of amino acid ester **11a** side product was observed in the crude reaction mixture (entries 2–4). The latter could be suppressed completely by using non-basic anion-containing tetraalkyl ammonium salts as the supporting electrolytes (entries 5–7) with Et_4N–BF_4 providing the highest yield of the desired **6a**. The anodic decarboxylation/cyclization reaction was similarly efficient when amount of water was reduced from 33% to 17% (entry 8 vs. 7), an observation that might be useful for substrates of low aqueous solubility. However, further reduction of water amount to 5 equivalents completely inhibited the anodic oxidation of **9a**, and only traces of the desired **6a** were observed (see SI, page S3). Decrease in supporting electrolyte concentration led to drop in yields (entry 9 vs. 8), whereas current density deviations from 12 mA/cm^2 did not affect the outcome of **6a** (see SI, page S4). Interestingly, replacement of graphite with stainless steel (SS) [9] as the cathode material afforded similar yields of the desired heterocycle **6a** (72% and 70%, respectively; entries 8 and 10), so both graphite and SS were subsequently used in the scope studies (*vide infra*). Other cathode materials such as Pt or BDD (boron-doped diamond) delivered **6a** in reduced yields (entries 11 and 12). Finally, brief examination of passed charge returned 2.0 *F* as the optimal amount. The amount of charge could be increased to 2.5 *F* in case of incomplete conversion of the starting **6a**, however further rise above 2.5 *F* led to a drop in pyrrolidine **6a** yield due to the formation of a new side product.

Table 1. Optimization of anodic decarboxylation/amidation reaction

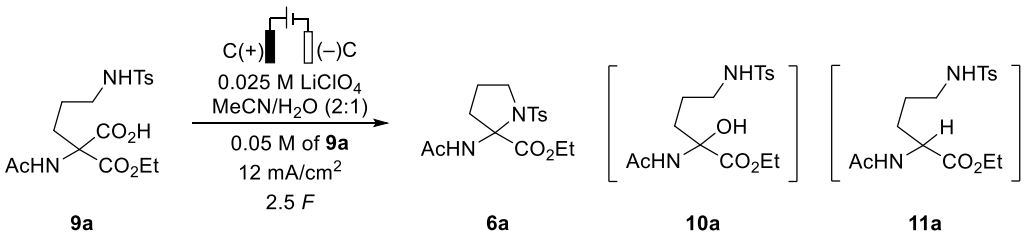

9a **6a** **10a** **11a**

Entry	Deviations from the starting conditions	Yield, %[a]	6a : 10a : 11a[b]
1	none	67	84:16:0
2	K_2CO_3, 2.0 *F*	54	86:3:11
3	Na_2CO_3, 2.0 *F*	54	86:4:10
4	NaOAc, 2.0 *F*	56	71:13:16
5	$Bu_4N–ClO_4$, 2.3 *F*	67	85:15:0
6	$Et_4N–PF_6$	66	85:15:0
7	$Et_4N–BF_4$	71	84:16:0
8	**$Et_4N–BF_4$, 5:1 MeCN/H_2O**	**72**	**86:13:1**
9	0.05 M $Et_4N–BF_4$, 5:1 MeCN/H_2O	67	85:13:2
10	**$Et_4N–BF_4$, 5:1 MeCN/H_2O, 2.0 *F*, SS (–)**	**70**	**87:13:0**
11	$Et_4N–BF_4$, 5:1 MeCN/H_2O, 2.0 *F*, Pt (–)	63	84:16:0
12	$Et_4N–BF_4$, 5:1 MeCN/H_2O, 2.8 *F*, BDD(–)	62	86:12:2

[a] Yields were determined by ^{1}H NMR post-electrolysis using CH_2Br_2 as an internal standard. The reactions were performed on a 0.15 mmol scale. [b] Ratios determined by LC-MS (UV detection).

We hypothesized that the side-product formation at increased amounts (>2.5 *F*) of passed charge results from undesired Shono oxidation of pyrrolidine **6a** [10,11]. Indeed, CV studies of **6a** revealed an irreversible feature at E_P = 1.78 V vs Ag/Ag^+ (100 mV/s scan rate; see Figure 3A), and the electrolysis of pyrrolidine **6a** under the optimized anodic decarboxylative cyclization conditions (entry 8, Table 1) afforded cyclic hemiaminal **12a (**33% NMR yield), which structure was proved by NMR experiments (Figure 3B). The relatively narrow potential window of 0.22 V between the desired decarboxylation in

9a (E_P = 1.56 V vs Ag/Ag^+) and the undesired Shono-type oxidation of the formed **6a** required careful control of the amount of passed charge to afford high yields of **6a**.

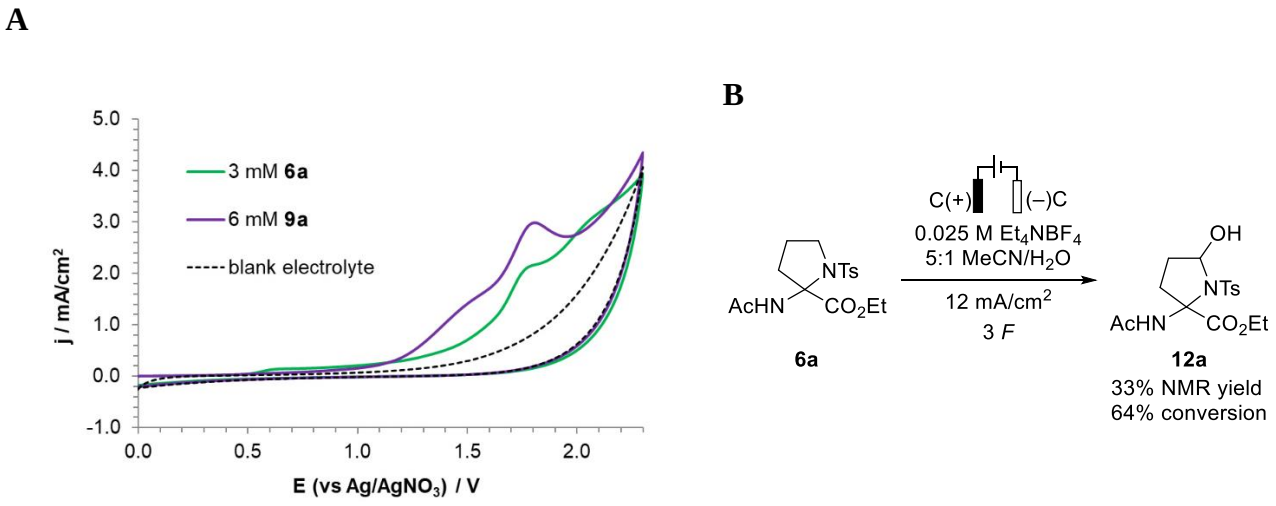

Figure 3. (A) Cyclic voltammograms of **6a** and **9a** at 3mM and 6 mM concentration, respectively, in 5:1 MeCN/H_2O (0.1M Et_4NBF_4). (B) Anodic oxidation of pyrrolidine **6a**

Next, the formation of decarboxylation product **11a** was addressed. Initially, we hypothesized that **11a** may form by a single-electron oxidation/decarboxylation (Kolbe reaction) of **9a** to generate carbon-centered radical, followed by hydrogen abstraction from solvent. To verify the hypothesis, electrolysis of acid **9d** was performed under optimized conditions (entry 10, Table 1) in deuterated solvents (Scheme 2; for details, see SI, page S40). Surprisingly, the electrolysis in the 5:1 mixture of MeCN-d_3 and water delivered **11d** without deuterium incorporation (Scheme 2, eq 1). In contrast, the formation of deuterated **11d-*D*** was observed by LC–MS when the electrolysis was performed in 5:1 MeCN/D_2O (Scheme 2, eq 2). The considerably higher O–H bond dissociation energy (119 kcal/mol) [12] as compared to that of C–H bond in MeCN (86 kcal/mol)[13] renders the hydrogen atom abstraction from water by carbon-centered radical a very unlikely mechanistic scenario. In the meantime, slow formation of **11d-*D*** was observed upon stirring of **9d** in the 5:1 MeCN/D_2O mixture even without applying electric charge (Scheme 2, eq 3). Apparently, **11d** was formed upon spontaneous loss of CO_2 from equilibrating deuterated carboxylate **9d-*D***. Furthermore, monoesters **9** are also prone to

spontaneous decarboxylation upon storage. Therefore, freshly prepared material should be used in the electrolysis.

An additional evidence against the single-electron oxidation/decarboxylation pathway (Kolbe electrolysis) for the formation of **11** was gained by a radical clock experiment (Scheme 2, eq 4) in which double bond-containing malonic acid monoester **9o** was subjected to anodic oxidation under the developed conditions in the presence of KOH (0.5 equiv). Unsaturated acids that are structurally related to **9o** have been reported to undergo facile radical 5-exo-trig cyclization under Kolbe electrolysis conditions [14,15]. However, the formation of a cyclic product **13** was not observed. Instead, hemiaminal **10o** was formed as the major reaction product together with decarboxylated compound **11o** (for details, see SI, page S48). Taken together, the control experiments provide strong evidence that the electrolysis of acids **9a**–**o** under the developed conditions most likely involves two-electron anodic decarboxylation and leads to the formation of a stabilized *N*-acyliminium ion intermediate.

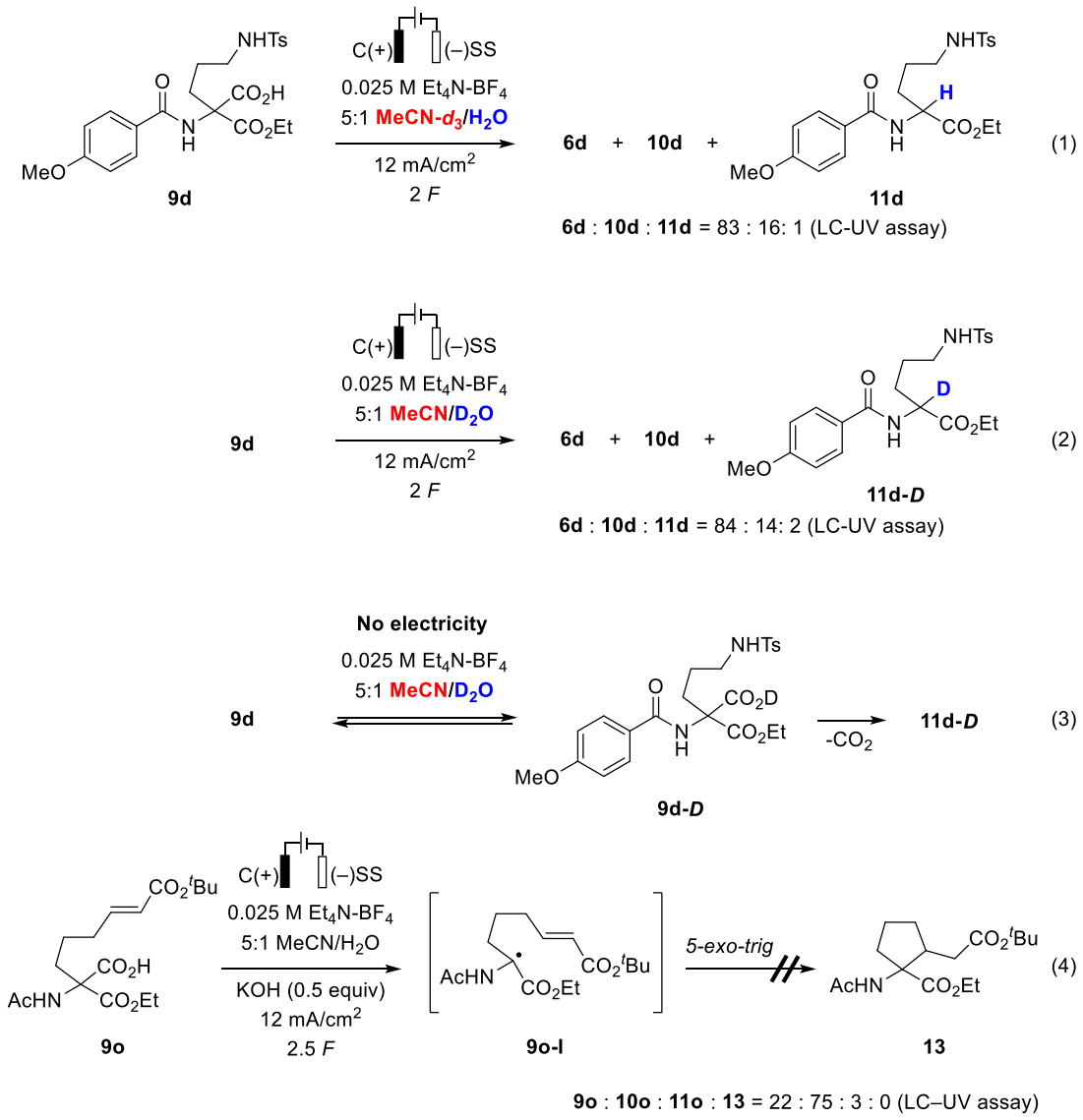

Scheme 2. Electrolysis of acid **9d** in deuterated solvents and the radical clock experiment

Based on experimental evidence, a working mechanism for the formation of 2-aminoproline **6a** is proposed (Figure 4). Accordingly, an initial deprotonation of carboxylic acid **9a** by cathodically generated hydroxide is followed by anodic oxidation/decarboxylation of the formed carboxylate **9a-I** to generate stabilized cation **9a-II**. The latter undergoes intramolecular cyclization with tethered *N*-nucleophile into cyclic aminal **6a**. In a competing reaction, the cation **9a-II** reacts with water to form acyclic hemiaminal **10a**.

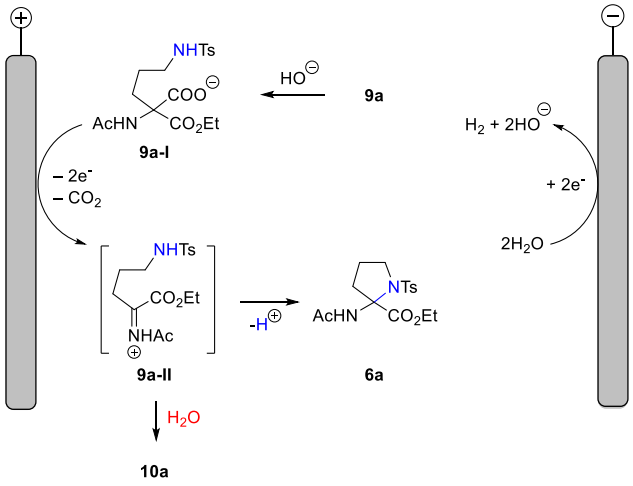

Figure 4. Plausible mechanism for formation of pyrrolidine **6a** and hemiaminal **10a**

With the optimized conditions in hand (Table 1, entries 8 and 10) the scope of the developed decarboxylative amidation was briefly explored (Table 2). *N*-Acetyl, *N*-Cbz, and *N*-Bz protecting groups are compatible with decarboxylation/cyclization conditions, and the respective 2-aminoproline derivatives **6a**–**c** were obtained in 49–75% yield. Redox sensitive 4-anisoyl and 4-cyanobenzoyl groups–containing monoesters **9d**,**e** are also suitable as substrates as evidenced by the formation of **6d**,**e** in 38–63% yields. Not only *N*-tosylates undergo the decarboxylative cyclization, but also *N*-mesyl–protected monoester **9f** could be converted into 2-aminoproline derivative **6f** in 60% yield using graphite cathode. However, *N*-*o*-nosyl–protecting group is not compatible with the developed electrolysis conditions, likely because it undergoes the undesired cathodic reduction. Indeed, trace amounts of 2-aminoproline derivative **6g** (<4%) could be obtained by replacing SS as the cathode material with platinum that has low overpotential for hydrogen evolution reaction [16]. To avoid the undesired cathodic reduction of the nitro group, the electrolysis of *N*-*o*-nosyl–protected monoester **9g** was performed in a divided cell in the presence of NaOH as a base (1 equiv). Gratifyingly, *N*-*o*-nosyl–protected **6g** was obtained in 25% yield.

The attempted synthesis of 2-amino pipecolic acid derivative **6h** under the developed conditions was unsuccessful, and afforded trace amounts of **6h** together with the corresponding acyclic hemiaminal **10h** as the major product. Such an outcome can be attributed to a slower formation of a 6-membered ring [17] from transient *N*-acyliminium species. Gratifyingly, the addition of KOH (1 equiv) to the electrolysis mixture facilitated the cyclization, and 6-membered heterocycles **6h**,**i** could be obtained in 27% and 18% yield, respectively.

In addition to sulfonamides, carbamates such as *N*-Boc and benzamide are also suitable as nucleophiles for the anodic decarboxylation/cyclization reaction. However, the corresponding 2-aminoproline derivatives **6j**,**k** were obtained in considerably lower yields (38%) as compared to those of *N*-Ts analog **6a**. Surprisingly, the addition of KOH (0.5 equiv) to the electrolysis solution has helped to improve yield of *N*-Boc-protected 2-aminoproline derivative **6j** from 38% to 59%. However, the addition of KOH was not always beneficial. For instance, the anodic oxidation of benzamide **9k** in the presence of KOH afforded pyrrolidine **6k** only as a minor product and a mixture of **6k**:**10k**:**11k** in 15:32:53 ratio, respectively, was formed. Finally, the loading of **9j** was increased from 0.3 to 2.7 mmol to demonstrate the scalability of the method, and 470 mg of 2-aminoproline derivative **6j** was obtained in a single electrolysis batch.

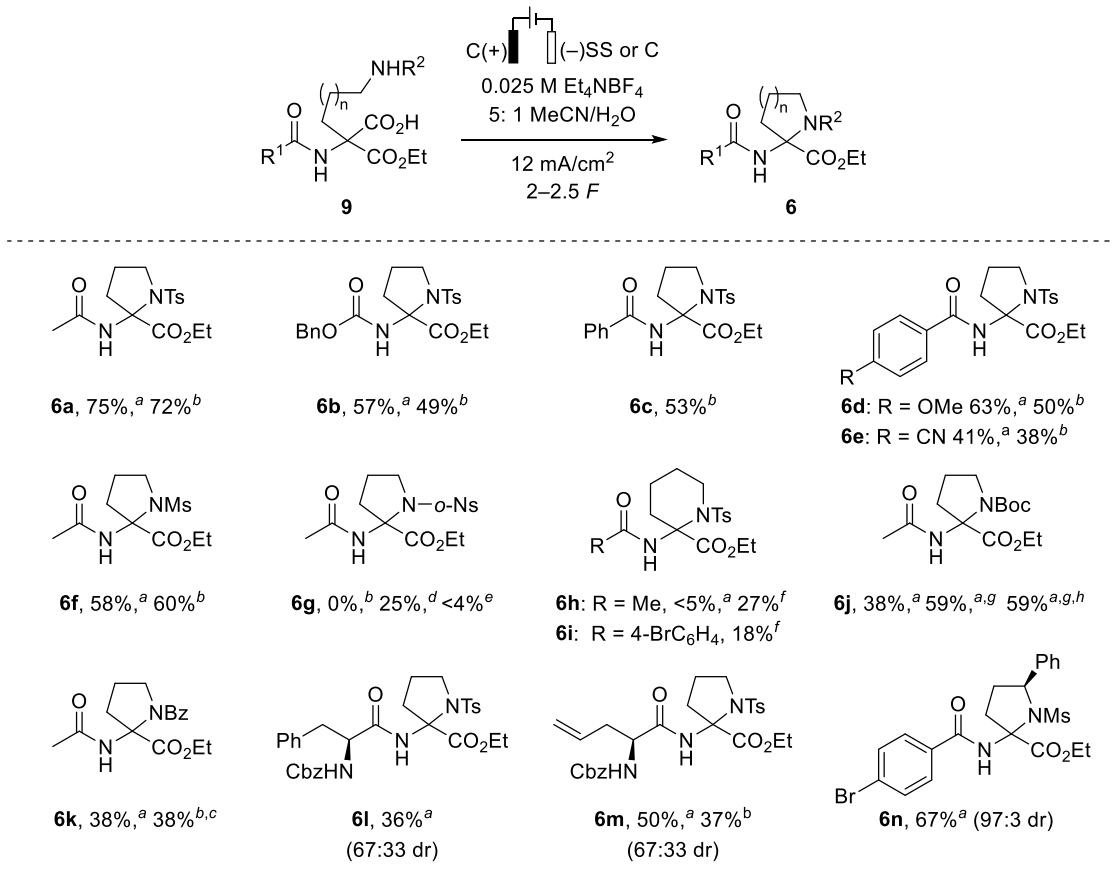

Table 2. Scope of decarboxylative amidation. [a] Stainless-steel cathode; [b] Graphite cathode; [c] Yield determined by NMR yield using CH_2Br_2 as an internal standard; [d] Electrolysis in divided cell with NaOH (1 equiv); [e] Pt cathode; [f] With KOH (1 equiv); [g] With KOH (0.5 equiv); [h] Performed at 925 mg (2.7 mmol) scale.

Wide application of unnatural amino acids in the design of peptidomimetics prompted us to examine the suitability of the developed conditions for dipeptide synthesis. Gratifyingly, the cyclization of amino acid fragment-containing monoesters **9l**,**m** afforded dipeptides **6l**,**m** in 36% and 50% yield, respectively. Notably, the decarboxylative cyclization is compatible with the alkene moiety (product **6m**). Both dipeptides **6l**,**m** were obtained as 67:33 mixture of diastereomers. In the meantime, excellent diastereoselectivity (97:3 dr) was achieved in the decarboxylative cyclization of *N*-mesylamide **9n** possessing *S* stereogenic center in α-position to the nitrogen. Unfortunately, the configuration of the newly formed quaternary stereogenic center in **6n** could not be established by NMR methods, and all attempts to obtain crystals suitable for X-ray crystallographic analysis were unsuccessful.

N-Protected 2-aminoproline derivatives **6** are relatively stable under basic conditions as evidenced by successful hydrolysis of ester moiety in **6a**,**d**,**e** using aqueous LiOH to provide acids **14a**,**d**,**e** in 71–83% yield (Scheme 3). Carboxylic acid **14a** could be reacted with glycine benzyl ester in presence of HATU and Et_3N to form dipeptide **17** (66%). In contrast, *N*-unprotected 2-aminoprolines are unstable and could not be isolated. Thus, the cleavage of *N*-Cbz protecting group in **6b** under Pd-catalyzed hydrogenolysis afforded diamino acid ester **15** (75% yield) that was likely formed by ring-opening of unstable *N*-unprotected 2-aminoproline followed by reduction of the open-chain imine tautomer. Likewise, the open-chain amino alcohol **16** was formed also upon the reduction of the ester moiety with $LiBH_4$. In the meantime, the hydrogenolysis of benzyl ester in dipeptide **17** proceeded smoothly and afforded carboxylic acid **18** in 81% yield (Scheme 3).

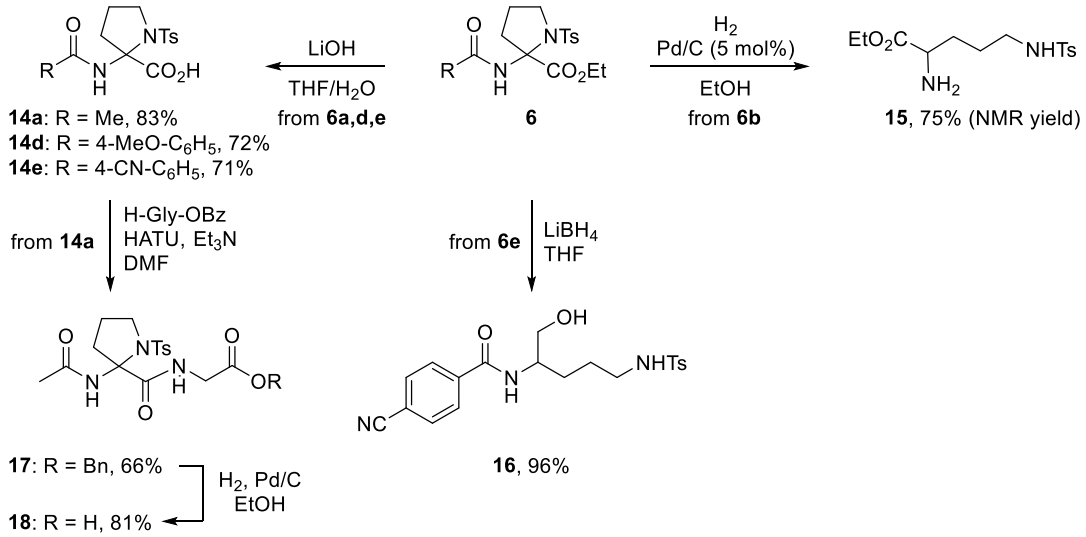

Scheme 3. Synthetic modifications of 2-aminoproline derivatives **6**.

Conclusions

In summary, the developed electrochemical decarboxylative amidation of readily accessible malonic acid monoesters provides an access to previously unreported 2-aminoproline derivatives. The decarboxylative amidation proceeds under constant current conditions in an undivided cell in aqueous acetonitrile and involves initial anodic decarboxylation followed by an intramolecular reaction of the formed stabilized cation with tethered nitrogen nucleophiles such as sulfonamides, carbamates, and benzamide. The decarboxylative cyclization of stereogenic center-containing sulfonamide proceeds with excellent diastereoselectivity (97:3 dr). The *N*-protected 2-aminoproline derivatives can be incorporated into dipeptides by ester hydrolysis/amide bond formation sequence, and therefore they are suitable for the design of peptidomimetics. Further work is in progress at our laboratory to expand the scope of nucleophiles in the decarboxylative functionalization of malonic acid monoesters.

Experimental

General procedure for electrochemical synthesis of pyrrolidines **6a**–**f**,**j**–**n** from the corresponding malonic acid monoesters **9a**–**f**,**j**–**n**.

An undivided electrochemical cell (5 mL, IKA ElectraSyn 2.0) was charged with starting carboxylic acid **9a**–**f**,**j**–**n** (0.2–0.3 mmol) and Et_4NBF_4 (0.025 M), followed by addition of MeCN (2.5 mL) and H_2O (0.5 mL). Graphite plate (8×52.5×2 mm; immersed electrode surface area A = 1.12 cm^2) was used as a working electrode and stainless steel or graphite (8×52.5×2 mm; immersed electrode surface area A = 1.12 cm^2) was used as a counter electrode. The electrolysis was carried out under galvanostatic conditions at room temperature, and 2.0 *F* charge (if not otherwise noticed) with current density of 12 mA/cm^2 was passed through the colorless reaction solution. The resulting clear, colorless (sometimes pale yellow) solution was concentrated under reduced pressure and the crude product was purified by column chromatography.

Cyclic voltammetry studies

CV experiments were carried out in an SVC-2 (ALS, Japan) three-electrode cell using a PalmSens4 (PalmSens). A glassy carbon disk (diameter: 1.6 mm) served as the working electrode, and a platinum wire as the counter electrode. The glassy carbon disk was polished using polishing alumina (0.05 μm) prior to each experiment. As a reference, $Ag/AgNO_3$ electrode [silver wire in 0.1 M NBu_4ClO_4/MeCN solution; c($AgNO_3$) = 0.01 M; E_0 = −87 mV vs Fc/Fc^+ couple] [18] was used, and this compartment was separated from the rest of the cell with a Vycor frit. Et_4NBF_4 (0.1 M, electrochemical grade) was employed as the supporting electrolyte in 5:1 MeCN/H_2O solution. The electrolyte was purged with argon for at least 3 min prior to recording. Compounds **6a** and **9a** were analyzed at a concentration of 3 mM or 6 mM and scan rate of 100 mV s^{-1}. The peak potential E_P was not extracted from background-corrected voltammograms. All CV graphs are plotted using IUPAC polarographic convention.

Supporting Information

Supporting Information File 1

Detailed experimental procedures, analytical and spectroscopic data for the synthesized compounds, and copies of NMR spectra.

Data Availability Statement

All data that supports the findings of this study is available in the published article and/or the supporting information of this article.

References

1. Blaskovich, M. A. T. *J. Med. Chem.* **2016**, *59*, 10807–10836. doi: 10.1021/acs.jmedchem.6b00319.
2. Gzik, A.; Borek, B.; Chrzanowski, J.; Jedrzejczak, K.; Dziegielewski, M.; Brzezinska, J.; Nowicka, J.; Grzybowski, M. M.; Rejczak, T.; Niedzialek, D.; Wieczorek, G.; Olczak, J.; Golebiowski, A.; Zaslona, Z.; Blaszczyk, R. *Eur. J. Med. Chem.* **2024**, *264*, 116033. doi: 10.1016/j.ejmech.2023.116033.

3 Pujala, B.; Panpatil, D.; Bernales, S.; Belmar, S.; Ureta Díaz, G. A. WO2020132661 A2, 2020.

4. Koleda, O.; Prane, K.; Suna, E. *Org. Lett.* **2023**, *25*, 7958–7962. doi: 10.1021/acs.orglett.3c02687.

5. Hawkins, B. C.; Chalker, J. M.; Coote, M. L.; Bissember, A. C. *Angew Chem Int Ed* **2024**, e202407207. doi: 10.1002/anie.202407207.

6. Sheng, T.; Zhang, H.-J.; Shang, M.; He, C.; Vantourout, Julien. C.; Baran, Phil. S. *Org. Lett.* **2020**, *22*, 7594–7598. doi: 10.1021/acs.orglett.0c02799.

7. Shao, X.; Zheng, Y.; Tian, L.; Martín-Torres, I.; Echavarren, A. M.; Wang, Y. *Org. Lett.* **2019**, *21*, 9262–9267. doi: 10.1021/acs.orglett.9b03696.

8. Yu, P.; Huang, X.; Wang, D.; Yi, H.; Song, C.; Li, J. *Chem.–Eur. J.* **2024**, e202402124. doi: 10.1002/chem.202402124.

9. Collin, D. E.; Folgueiras-Amador, A. A.; Pletcher, D.; Light, M. E.; Linclau, B.; Brown, R. C. D. *Chem.–Eur. J.* **2020**, *26*, 374–378. doi: 10.1002/chem.201904479.

10. Shono, T.; Matsumura, Y.; Tsubata, K.; Uchida, K.; Kanazawa, T.; Tsuda, K. *J. Org. Chem.* **1984**, *49*, 3711–3716. doi: 10.1021/jo00194a008.

11. Novaes, L. F. T.; Ho, J. S. K.; Mao, K.; Liu, K.; Tanwar, M.; Neurock, M.; Villemure, E.; Terrett, J. A.; Lin, S. *J. Am. Chem. Soc.* **2022**, *144*, 1187–1197. doi: 10.1021/jacs.1c09412.

12. Benson, S. W. *J. Chem. Educ.* **1965**, *42*, 502. doi: 10.1021/ed042p502.

13. Kerr, J. A. *Chem. Rev.* **1966**, *66*, 465–500. doi: 10.1021/cr60243a001.

14. Lebreux, F.; Buzzo, F.; Markó, I. *Synlett* **2008**, 2815–2820. doi: 10.1055/s-0028-1083547.

15. Newcomb, M.; Varick, T. R.; Ha, C.; Manek, M. B.; Yue, X. *J. Am. Chem. Soc.* **1992**, *114*, 8158–8163. doi: 10.1021/ja00047a026.

16. Hickling, A.; Salt, F. W. *Trans. Faraday Soc.* **1940**, *36*, 1226–1235. doi: 10.1039/TF9403601226.

17. Di Martino, A.; Galli, C.; Gargano, P.; Mandolini, L. *J. Chem. Soc., Perkin Trans. 2* **1985**, 1345. doi: 10.1039/p29850001345.

18. Pavlishchuk, V. V.; Addison, A. W. *Inorg. Chim. Acta* **2000**, *298*, 97–102. doi: 10.1016/S0020-1693(99)00407-7.